

# Analysis of Distributed Deep Learning in the Cloud

Aakash Sharma

The Pennsylvania State University  
abs5688@psu.edu

Rishabh Jain

The Pennsylvania State University  
rishabh@psu.edu

Mahmut Taylan Kandemir

The Pennsylvania State University  
mtk2@psu.edu

Vivek M. Bhasi

The Pennsylvania State University  
vmb5204@psu.edu

Jashwant Raj Gunasekaran

Adobe Research  
jgunasekaran@adobe.com

George Kesidis

The Pennsylvania State University  
gik2@psu.edu

Sonali Singh

The Pennsylvania State University  
sms821@psu.edu

Subrata Mitra

Adobe Research  
subrata.mitra@adobe.com

Chita R. Das

The Pennsylvania State University  
cxd12@psu.edu

## ABSTRACT

Deep neural networks (DNNs) have become popular owing to their ability to solve complex problems such as image recognition, autonomous driving, natural language processing, etc. Their growing complexity coupled with the use of larger volumes of training data (to achieve acceptable accuracy) has warranted the use of GPUs and other accelerators. Such accelerators are typically expensive, with users having to pay a high upfront cost to acquire them. For infrequent use, users can, instead, leverage the public cloud to avoid the high acquisition cost. However, with the wide diversity of hardware instances (particularly GPU instances) available in public cloud, it becomes challenging for a user to make an appropriate choice from a cost/performance standpoint.

In this work, we aim to resolve this problem by introducing a comprehensive distributed deep learning (DDL) profiler, which can determine the various execution "stalls" that DDL suffers from while running on a public cloud. We have implemented the profiler by extending prior work to additionally estimate two types of communication stalls - interconnect and network stalls. We train popular DNN models using the profiler to characterize various AWS GPU instances and list their advantages and shortcomings for users to make an informed decision. We observe that the more expensive GPU instances may not be the most performant for all DNN models and AWS may sub-optimally allocate hardware interconnect resources. Specifically, the intra-machine interconnect can introduce communication overheads up to 90% of DNN training time and network-connected instances can suffer from up to 5 $\times$  slowdown compared to training on a single instance. Further, we model the impact of DNN macroscopic features such as the number of layers and the number of gradients on communication stalls. Finally, we propose a measurement-based recommendation model for users to lower their public cloud monetary costs for DDL, given a time budget.

## 1 INTRODUCTION

The continual growth of deep learning has fuelled many facets of Artificial Intelligence such as machine vision [52], speech [31], autonomous driving [26], natural language processing [14], etc. The advancements in deep learning have mainly been driven by availability of large amounts of training data as well as powerful compute platforms such as CPU or GPU clusters [7, 8], TPUs

[63], NPUs [18] and other accelerators that can handle increasingly complex Deep Neural Network (DNN) computations. However, the ever-growing DNN-model and training data sizes accompanied by the increasing ubiquity of DNNs places a higher demand on compute resources for faster processing speeds and shorter overall training time. Although current accelerators enable faster training, they are typically expensive to maintain, owing to their power-hungry nature, thereby, potentially rendering them cost ineffective, especially in intermittent training scenarios. To avoid the prohibitively high upfront cost of purchasing a GPU machine/cluster, users employ public cloud GPU resources [7, 8] to run their workloads.

Public cloud providers such as AWS [5], Azure [46] and GCP [20] provide a gamut of GPU instance offerings. These offerings vary in their hardware configurations and pricing. Cloud providers typically do not allow any flexibility in changing the CPU vCores, memory or GPUs of an instance, limiting users to select a best available "pre-configured" instance. Note that the choice of instance type(s) drives the total cost of training a model [11] and users have to rely on benchmarks such as DawnBench [11], NVIDIA examples [50], etc. or on their intuition to choose the type of instance(s). While users can choose a single instance with a single GPU for cost effective training, the long running time of deep learning makes it impractical. Moreover, the public cloud offers different types of GPUs to choose from and many users are at a loss when deciding which GPU is the most performant and/or cost effective for their model. For deep learning, users typically base their decisions on online articles, blogs, user manuals, and generic cost management tools, often created by cloud providers themselves.

To resolve this problem, we introduce a Distributed Deep Learning (DDL) profiler STASH, which is built upon the DS-analyzer profiler [16] released by Microsoft fiddle [47]. DS-analyzer introduced by Mohan et al. [44] characterizes DNN jobs in the Microsoft production cluster with emphasis on the stalls suffered due to CPU pre-processing and storage I/O latency. However, we observe communication overhead to be the primary contributor to DDL, which is also corroborated by prior work [48, 62]. This is not considered by DS-analyzer. Hence, we extend upon existing work by focusing on communication overheads, i.e., the interconnect and network stalls (or communication stalls) incurred during DDL.

We propose novel techniques to profile the communication-related stalls and implement it as part of our profiler. Using our

profiler, we then extensively characterize public cloud instances for the various stalls they suffer from by running popular DNN models on them. Characterizing such stalls on a public cloud (AWS in our experiments) is particularly useful, as various offerings differ not just in the hardware they offer, but also in the QoS that they provide, as discussed in later sections. Also, a systematic study of the communication overhead of public cloud instances for DDL is lacking, partly due to the lack of publicly-available tools or profiling methodologies to measure such an overhead. We attempt to bridge this gap by carefully measuring the interconnect and network stalls on various GPU-accelerated instances of a public cloud during DDL. Further, using this profiler, we analyze a number of DNN architectures to understand which architectural properties (such as the number and sizes of layers) drive communication stall behavior. And finally, we build a recommendation model for a prospective user (AWS user in our example) that would enable them to choose more efficient instance types, i.e., for a given training time budget (user’s SLO), our proposed model will recommend an appropriate type and number of instances for their DDL job while minimizing the associated monetary cost<sup>1</sup>.

Our **main contributions** in this paper are summarized below:

- We introduce STASH, a profiling tool which can measure interconnect and network stalls, in addition to CPU and storage stalls, of DDL workloads on any compute cluster.
- We perform stall analysis on various AWS GPU instances, using a number of popular DNN models. The estimated communication overhead from intra-machine interconnect was found to be up to 90% of the training time and network-connected instances were found to slow down by up to 5× compared to a single instance.
- We identify the limitations of each instance type. Specifically, our results indicate that higher capacity GPU instances don’t always lead to better performance and that AWS hardware interconnects have various shortcomings.
- We identify architectural features in DNN models that influence communication stall behavior, in particular the number of layers in addition to the total number of parameters (size of the DNN model).
- Finally, we build a recommendation model, which along with STASH, can find the most (monetary) cost-effective instance(s) for DDL. The model extrapolates based on actual AWS measurements taken by STASH.

The rest of this paper is organized as follows. In section 2, we discuss the background pertinent to DDL, AWS GPU instances, and DS-Analyzer. In section 3, we motivate our problem. Our characterization scheme is described in section 4. The results of our characterization are given in sections 5 and 6 along with the recommendation model. In section 7, we provide an overview of all the related work in this area. Finally, section 8 summarizes our findings.

## 2 BACKGROUND

Several distributed training methods have been proposed to parallelize the computations on multiple machines. These distributed deep learning (DDL) techniques broadly fall under two categories:

<sup>1</sup>Alternatively, one could minimize execution time subject to a monetary cost budget.

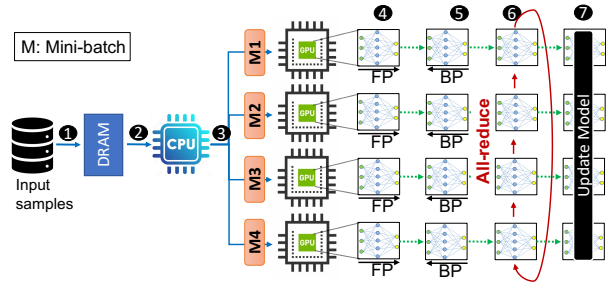


Figure 1: A typical Distributed DNN training pipeline.

data parallel [38] and model parallel [12] training. In the former, the model is replicated and data is partitioned across multiple devices for parallel computation, whereas in the latter, the model is split into multiple partitions, which are processed on different GPU devices. We limit the scope of this work to studying data parallel DDL, since extending STASH to model parallelism would be a work in its own right. We leave this for future work. In this section, we summarize the main steps involved in data parallel training and then provide an overview of the different public cloud offerings of AWS for running the DNN workloads.

### 2.1 Data-Parallel Distributed Deep Learning

Figure 1 outlines the typical process of distributed DNN training (deep learning) where several epochs comprising multiple iterations are performed. For each of these iterations, mini-batches of data items (training samples) are first fetched from storage (1). These data items are then pre-processed to make them amenable to training (2). To perform training, the data items are first partitioned among all workers (GPUs) where each holds a copy of the DNN model (3). Each worker then performs a forward pass (FP) to obtain the model’s current prediction on its partition and a loss value is calculated depending on its deviation from the ground truth (4). Next, each worker performs a backward pass (BP) to compute the gradients of the loss function with respect to the model parameters (weights) (5). This is followed by a synchronization step wherein the weight gradients are exchanged (communicated) and aggregated across all workers via a collective all-reduce operation (6). Finally, the optimized weight updates are calculated using these aggregated weight gradients which are applied to all models in parallel (7), after which the same steps are repeated for the next iteration.

Note that, in the above procedure, the different steps are primarily associated with specific hardware components. For instance, step 1 involves storage I/O, step 2 is typically CPU-bound, while steps 3, 4, 5, 6 and 7 are GPU-bound. Additionally, while performing the weight gradient aggregation (6) and sometimes even during BP (5), the gradients are communicated amongst the workers either using interconnects (such as PCIe and NVLink) and/or network links (such as Ethernet and Infiniband).

### 2.2 Public Cloud Offerings

Hardware capabilities, both in terms of compute and interconnects, are particularly significant in the context of DDL on the public cloud, as the GPU instances offered by providers (such as AWS) have fixed

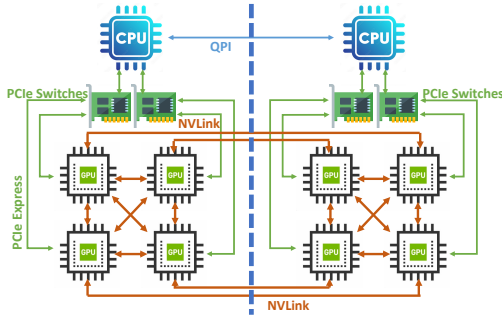


Figure 2: P3.16xlarge interconnect architecture.

configurations [6], thereby limiting user choice of a custom single-node training solution. Table 1 presents the GPU instance types offered by AWS along with some hardware specifications and their pricing. The P4 instances have the most powerful GPUs (NVIDIA A100 Tensor core GPUs), while the P3 and P2 instances respectively have the less powerful, yet quite capable, NVIDIA V100 and K80 GPUs. The P3 and P2 instances are of particular interest to us, as they offer the most variety in terms of number of GPUs available per node amongst all GPU instances viable for DNN training<sup>2</sup>.

Apart from the GPUs used, the interconnects and network links available to these instance types also have a significant impact on the end-to-end training time as they dictate data transfer speeds during various training steps. Specifically, interconnect links are utilized during gradient communication among workers (GPUs) present on the same physical node whereas network links are used when the communication is between workers on different nodes. The interconnect architecture for the AWS P3.16xlarge instance [32] is depicted in Figure 2.

We aim to demonstrate in this work that choosing the optimal instance configuration from these offerings to maximize performance, while minimizing cost, is a non-trivial problem as various factors, including GPU type, core count, number of instances, interconnects/network links used, and DNN model type can all play crucial roles in determining this. Further, we perform characterization on possible instance configurations (distributed and single-node) to identify training bottlenecks and accordingly suggest near-optimal configurations to the user.

Instance type(s)	GPUs	VCPUs	Interconnect	Network Bandwidth (Gbps)	Price/hr	
P4	8×A100	96	NVSwitch	400	\$32.7726	
P3	p3.2xlarge	1×V100	8	PCIe	up to 10	\$3.06
	p3.8xlarge	4×V100	32	PCIe + NVLink	10	\$12.24
	p3.16xlarge	8×V100	64	PCIe + NVLink	25	\$24.48
P2	p2.xlarge	1×K80	4	PCIe	< 10	\$0.90
	p2.8xlarge	8×K80	32	PCIe	10	\$7.20
	p2.16xlarge	16×K80	64	PCIe	25	\$14.40

Table 1: AWS GPU instance types with prices (N. Virginia).

<sup>2</sup>P4 is a bare metal offering not considered herein

### 2.3 DS-Analyzer: Stall Characterization

Among the works that characterize the private cloud [3, 4, 25, 29, 33, 45], DS-Analyzer[44] is of particular significance to us as it also aims to identify DNN training bottlenecks, specifically with regards to ‘fetch’ and ‘prep’ stalls. These stalls refer to the time spent fetching mini-batches of data from the disk (fetch stall) and pre-processing it prior to training with it (prep stall) in a deep learning iteration.

DS-Analyzer uses three steps to calculate prep and fetch stalls (refer to Figure 4). Step ② pre-populates synthetic data in the GPUs and runs training to measure the maximum ingestion rate of the system. This is followed by step ③ which runs training on actual data but with all OS caches cleared<sup>3</sup>. Finally, in step ④, training is run over actual data such that the entire data is cached in main memory (from the previous step). The prep stall is calculated by finding the difference between ④ and ①. This is because there is no storage I/O involved in step ④ and any difference in training time after deducting the time spent in GPU processing of ① will yield the time spent in pre-processing at CPU. After this, the fetch stall is calculated by finding the difference of ③ and ④, since any increase in time over ④ would be due to storage I/O.

### 3 DDL STALL ANALYSIS IN PUBLIC CLOUD

In this section, we highlight the novelty of this work over prior work. Further, we motivate the importance of profiling communication stalls in DDL especially on the public cloud.

#### What are the limitations of prior work?

As stated earlier, [16] profiled DDL jobs in the Microsoft cluster for CPU and disk stalls. However, there are several limitations in this work including not considering communication stalls. Further, the characterization was done on a private cluster with little hardware architecture details available. While the readers can learn about data stalls in DDL from this work, the work is of little use to public cloud users where hardware configurations are fixed.

#### Are there prior work which analyze communication overhead in DDL?

In [48], the authors measure the communication overhead of training to be 80% of the entire training time as part of their motivation study. But they did not specify any general methodology to measure overhead. [62] characterized DDL workloads on Alibaba PAI [10] and found communication overhead to be 62% with the use of parameter server (PS) [37] whose communication performance is strictly less than all-reduce [36, 62]. Moreover, the work was done in a private cluster and specific hardware details of the machines running the workload were not released. Although they have released a general profiling methodology using TensorFlow [1] internal tooling and manual feature extraction, it is limited to TensorFlow and the PS communication architecture. Finally, [39] characterize DDL training on the Google Cloud but do not specifically measure communication overhead. They build a general framework for measuring DDL performance but specifically for transient cloud instances which are frequently revoked. We list other works in section 7.

<sup>3</sup>In the original paper, this step is described to be after the next step but we observed from the DS-analyzer open source code that that is not the case.

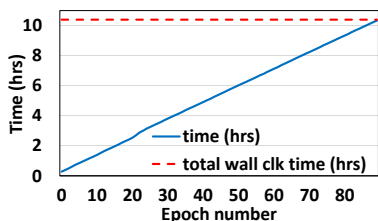


**Figure 3: End-to-end ResNet18 training time on ImageNet vs. number of epochs. Training time scales linearly with #epochs.**

### Why Profile Communication Overhead in DDL?

To reduce the communication overhead of DDL, several distributed DNN algorithms have been proposed [13, 21, 24, 37, 40, 68, 69]. However, there is a lack of a *profiling tool* to measure the specific efficacy with regards to communication overhead for various algorithms. Even when the efficacy study exists for specific algorithms, ML scientists lack the tools to measure various communication overheads that their optimizations may suffer from. An ML scientist may remain oblivious to the slowdown caused by communication links on their otherwise high-performing algorithm with a single GPU.

### Why Characterize GPU Instances of Public Cloud?

The gamut of public cloud GPU-based instances available (Section 2.2) makes the task of choosing the most performant configuration a non-trivial one for end users. This is due to a lack of a proper scientific study that characterizes the various public cloud GPU instances. Prior work on characterizing deep learning such as [3, 4, 25, 29, 33, 39, 44, 45, 62] do not characterize instances of the public cloud for their QoS and users cannot use these works to choose appropriate instance type(s). To make matters more complex, cloud providers offer different types of interconnects for their GPU-accelerated instance type(s). Apart from the interconnect type, the user can also "tie" the various instances through the computer network. These communication options introduce further complexity to the choice of instance(s) for DDL. In the absence of a characterization and profiling technique for choosing instance type(s), users can only guess the best instance to run their AI workload based on marketed hardware configurations from the cloud provider.

### How to Lower the Training Cost on Public Cloud?

For a typical DNN user, the cost of running training is an important metric to consider when using the public cloud, i.e., "cloud-spend" [65]. And, the choice of the public cloud instance(s) is the most important factor determining the cost of DDL. In this work, we try to answer this question by characterizing various AWS P instance types with regards to their "stall behavior" during DDL. We also identify the features in the DNN architecture which impact the communication stalls observed in training. And finally we build a recommendation model to lower the training cost.

## 4 METHODOLOGY

In this work, we use AWS public cloud to run all our experiments. Specifically, all our experiments are run in the AWS N. Virginia

region using the AWS P instance type which is AWS's recommended instance type to run deep learning.

Using our profiler STASH, we characterize various AWS P instances with reference to four stall parameters, namely: (i) CPU stall (prep stall), (ii) Disk stall (fetch stall), (iii) Interconnect stall, and (iv) Network stall. While these stall quantities provide important insights into the hardware characteristics of AWS instances, we also provide a training time and monetary cost comparison of running DDL on various AWS instance types. Our characterization exploits the repetitive nature of deep learning and is able to calculate the various stalls from a single epoch. This is possible since a single epoch is representative of the training time which scales linearly with the number of epochs. Consider the plot of training time vs. epoch number during end-to-end training of a ResNet18 DNN [23] on the ImageNet dataset [28] in Figure 3. The model was trained for 90 epochs with a batch size of 1024 in a distributed data parallel regime on a cluster of 4 NVIDIA A100 GPUs. Upon conclusion of training, the top-1 and top-5 validation accuracies respectively were 67.5% and 87.8%. As can be seen from the figure, the training time increases linearly with the number of epochs and the total training time (obtained as a sum of per-epoch training time over 90 epochs) matches the wall-clock time of training. Hence, we conclude that a single epoch is representative of the entire training time and is sufficient for our characterization study.

### 4.1 Characterization

We conduct two types of characterizations, macro and micro, as explained below.

**Macro Characterization:** We profile DDL consisting of both small and large models as workloads to characterize the relevant AWS GPU instances. The small models consist of ResNet18 [23], AlexNet [34], MobileNet-v1 [58], SqueezeNet [27], and ShuffleNet [43]. The large models include ResNet50 [23] and VGG11 [59]. The input dataset for these models is ImageNet 1k [28]. All our experiments are run across four batch sizes with the highest batch being the maximum batch size supported by the GPU.

**Micro Characterization:** We conduct micro characterization by running synthetic training experiments on two models – ResNet and VGG. As part of this, we study various aspects of the model architecture that influence communication stalls including the number of layers. We also tweak certain model architecture features (such as "residual" network branches and batch normalization layers) to study their impact on communication stalls.

### 4.2 Profiler Design

A schematic view of the STASH profiler is depicted in Figure 4. As mentioned earlier, STASH is an extension of the DS-Analyzer profiler. In the figure, step ① and step ⑤ have been added to calculate communication stalls and steps ②③④ were pre-existing as part of the DS-Analyzer. STASH pre-populates the GPU memory with synthetic training data as part of step ①.② and ⑤ and runs training over it. Training over synthetically pre-populated data has the unique advantage of eliminating all CPU and disk stalls as neither disk I/O nor CPU pre-processing are happening while training. However, since training is run using multiple GPU workers, it is still bound to suffer from communication stalls. Below, we describe



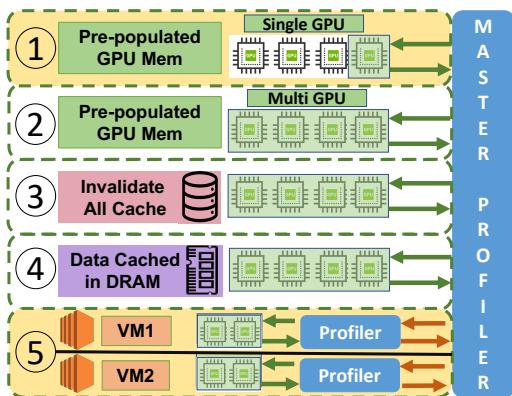


Figure 4: High level view of the STASH profiler

the methodology of determining the communication stalls using step ① and step ⑤.

**4.2.1 Interconnect Stall.** We define an interconnect stall as the *inter-GPU communication overhead of DDL in a single machine that arises due to the communication among the GPUs*. This is a key indicator of the performance of the underlying interconnect and is suggestive of the adverse impact this can have on end-to-end training time. We determine the interconnect stall in two steps:

- (1) STASH pre-populates synthetic data in the memory of a single GPU only such that the number of samples the GPU processes is the same as a single GPU in a distributed training with multiple GPUs. The batch size for multi-GPU training is kept the same as that of a single GPU. STASH then performs synthetic training on just a single GPU (in a multi GPU machine) while keeping all other GPUs idle; see step ① in Figure 4. Since this is a single-GPU training, no inter-GPU communication overhead is incurred.
- (2) STASH then runs distributed training over all GPUs in the machine on synthetic data. The number of samples each GPU processes and the per GPU batch size is kept the same as in step ①.

Note that distributed training adds communication overhead to the end-to-end training time as a consequence of gradient synchronization. Hence, the difference in training time between ② and ① essentially yields the interconnect stall of the model for a particular machine.

We now describe an example of determining interconnect stalls using Figure 5. Suppose in a four GPU machine, the total DNN training data set consists of  $n$  samples and the training must run over four mini-batches per epoch as the batch size per GPU is set as  $n/4/4$ . Therefore, as part of ①, STASH will pre-populate only one GPU with  $n/4$  samples and a training process will be launched for one epoch using that particular GPU, keeping the other GPUs idle. This single-GPU training epoch has no need for gradient synchronization and hence does not suffer from communication overhead as described in the figure. After step ①, STASH will pre-populate all other GPUs with  $n/4$  samples each as part of step ② and launch distributed training over  $n$  samples (i.e., a DDL epoch). These

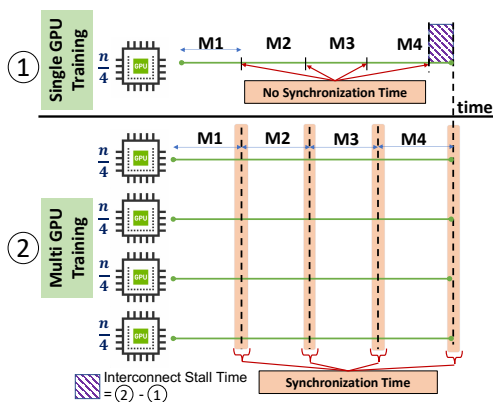


Figure 5: Interconnect stall calculation (M: Mini-batches, batch size =  $n/4/4$ ).

four training processes will suffer from communication overhead due to the all-reduce (gradient synchronization) step as described in the figure. The difference between the elapsed time of training over  $n$  samples with 4 GPUs and training over  $n/4$  samples with a single GPU is the communication overhead time (indicated in figure), which is essentially the interconnect stall.

**4.2.2 Network Stall.** We define a network stall as the *inter-GPU communication overhead of DNN training over multiple machines that arises due to the network link(s) between them*. This type of stall occurs when DDL is performed across multiple machines linked through computer networks. Since the all-reduce step requires gradients to be sent via both the intra-machine interconnect network as well as the inter-machine computer network, the slowest link becomes a communication bottleneck. Whenever the network link is the slowest link, network stalls occur. STASH determines network stalls as follows. Synthetic distributed training is run over multiple machines connected via network such that the total number of GPUs is the same as in the single machine training of ②. This is step ⑤ of Figure 4. The difference between the training times of ② and ⑤ yields the *network stall* of the model.

Again, we describe an example of determining a network stall using Figure 6. Suppose we run step ② in an instance with 4 GPUs over  $n$  data samples as shown in the figure. As part of ⑤, STASH now runs training over 2 instances with 2 GPUs each but with  $n/2$  samples per machine keeping the per GPU batch size same. When we train over 2 instances with a network link between them, the communication is bottlenecked over the network link if the link is slower than the hardware interconnect (most cases). For most cases where the network link is slower than the hardware interconnect, the network stall of the system is calculated as the time difference between ② and ⑤.

## 5 MACRO CHARACTERIZATION

The characterization starts by asking two fundamental questions for DDL jobs: (i) **which instance type is the most cost effective?**, and (ii) **which instance type is the most performant?** To answer these two fundamental questions, we realize that further

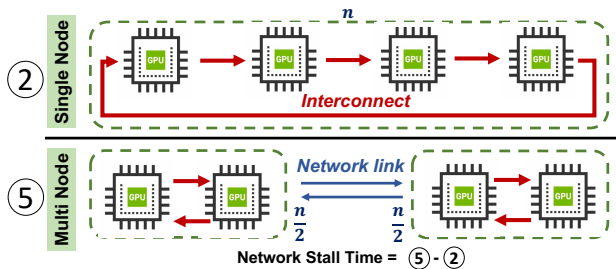


Figure 6: Network stall calculation.

specific questions need to be asked including stall times of various hardware resources. We begin our discussion by asking a simple but specific question: How much stall do DDL jobs experience from four hardware resources – CPU, disk, interconnect and network? Answering this question will enable us to pinpoint the specific hardware characteristics of an instance that leads to job slowdowns. To answer the above questions, we conduct a stall analysis on AWS P type instances while keeping the GPU as the first class resource and base our answers through the resource requirements of representative DDL workloads. While we use specific DNN models as example workloads, the techniques used here can be generalised to all DDL workloads. For each example workload, STASH performs four different runs with increasing batch sizes as explained in section 4. But the highest batch size is the largest per-GPU mini-batch size that fits in GPU memory. The batch size stated in the figures is per GPU and the effective batch size is the per GPU batch size times the number of GPUs. In the interest of space, we only show the plots of the smallest and largest batch sizes in the paper. Our discussion starts in the sequel.

### 5.1 Analysis on AWS P2

AWS P2 instances use the NVIDIA K80 GPU with PCIe third generation interconnects. The P2 instances consist of three instance types – P2.xlarge, P2.8xlarge and P2.16xlarge as discussed in section 2. We profile P2 instances with models AlexNet, ResNet18, ShuffleNet\_v2, MobileNet\_v2 and SqueezeNet across four mini-batch sizes – 32, 64, 96 and 128. Since K80 GPUs have limited compute and memory resources, they are not very suitable for running large models, i.e. models with a high parameter count. In practice, we observed very high stalls and monetary cost of running large models on P2 instances compared to P3. As a result, we employ the smaller models to characterize stalls on the K80 GPUs.

**5.1.1 Stall Analysis.** Figure 7 shows the CPU and disk stalls as a percentage of the total training time for mini-batch sizes 32 and 128. Unlike ref. [44], we notice negligible CPU stalls in AWS, pointing to the fact that vCPUs at AWS are sufficient for most pre-processing needs of DL jobs. This goes against the common wisdom that AWS offers lower QoS in their CPU throughput. We further notice the largest amount of disk stalls for the 16x type machine. This is because there are 16 data loading workers running on the 16x machine to exploit the 16 GPUs of the machine. The 16 workers read from the attached SSD in parallel and create an I/O contention. The AWS general purpose SSD used in our experiments is unable

to keep up with this demand and the training spends a significantly long time in disk stalls.

We now discuss the interconnect and network stalls of P2 instances. We observe from Figure 9(b) that the 16x large runs a slower training than two 8xlarge machines that are network connected. This is true in all our batch runs. Further, we observe from Figure 8 that 16xlarge has a higher interconnect stall time than both 8xlarge and 8xlarge\*2 (two 8xlarge). Two 8xlarge instances connected via the network do not suffer from any network stalls as they are faster than the 16xlarge. So, **what is causing the slowdown in the 16xlarge?**

The reason for this slowdown in 16xlarge is that P2 instances use PCIe bus for communication which has limited bandwidth. In case of 16xlarge, the PCIe bandwidth is shared among 16 workers causing congestion and "slicing" of the limited PCIe bandwidth. We test this theory by finding the PCIe bandwidth using CUDA in xlarge, 8xlarge and 16xlarge instances. All GPUs are used in parallel when running the bandwidth test and we report the per device bandwidth in Figure 10.

As is clear from the figure, the GPUs in 16xlarge instance receive significantly less bandwidth than the GPUs of all other P2 instance types. This bandwidth is lower than the expected network bandwidth and hence the training gets throttled on the interconnect link, rather than on the network. As the network is not the slowest link and 8xlarge instance has access to higher interconnect bandwidth than the 16xlarge, the 8xlarge\*2 configuration performs better than the 16xlarge. This gives us an intuition that the 16x instance is the least cost optimal and we test this hypothesis empirically by checking the monetary cost of running the workloads.

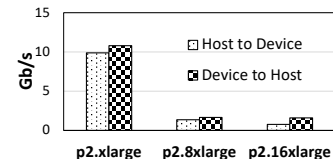


Figure 10: Per GPU PCIe bandwidth measured in P2

We show the dollar cost comparison of all P2 instances in Figure 9(a). A linear increase in cost is observed as the size of the P2 instance is increased. This confirms the hypothesis from our study of interconnect stalls that as the interconnect stalls increase, the monetary cost of performing the same DDL workload also increases. The lowest cost of running the training is on P2.xlarge which has a single GPU and hence has no interconnect stalls. However, the DDL execution time doesn't always decrease linearly from smaller instance to larger instance.

We again notice from Figure 9(b) that there is no significant improvement in training time on 16xlarge for a 2x increase in cost. In fact, we notice in most cases that the running time in 16xlarge is more than that of 8xlarge, although the instance has twice the resources of 8xlarge. This is because although resources like CPU, GPU and memory are doubled, the PCIe bus bandwidth remains the same as already demonstrated causing congestion and significant slowdowns.

**5.1.2 Recommendation.** We experience both high interconnect and disk stalls on the 16xlarge instance and accordingly recommend to not use the 16xlarge instance. Even when more GPUs are needed

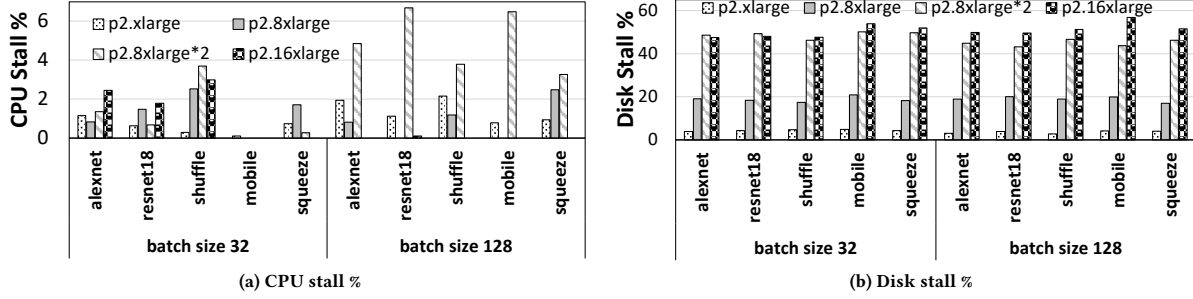


Figure 7: CPU and disk stall %age of total training time (P2).

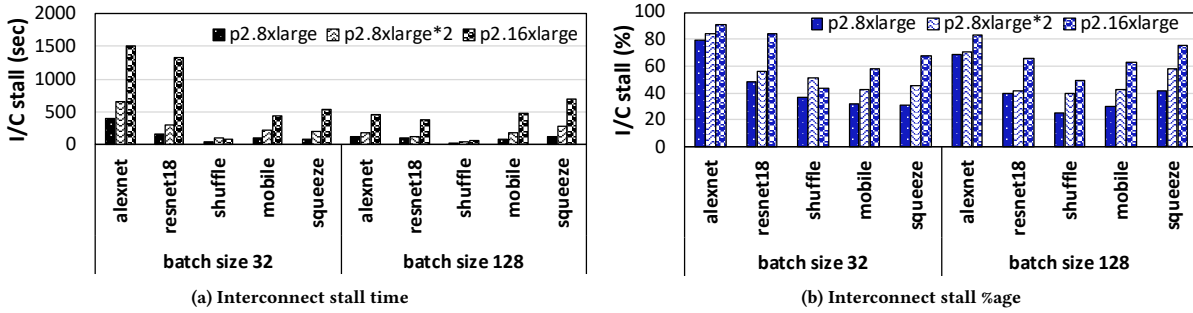


Figure 8: Interconnect Stall (P2, Small Models)

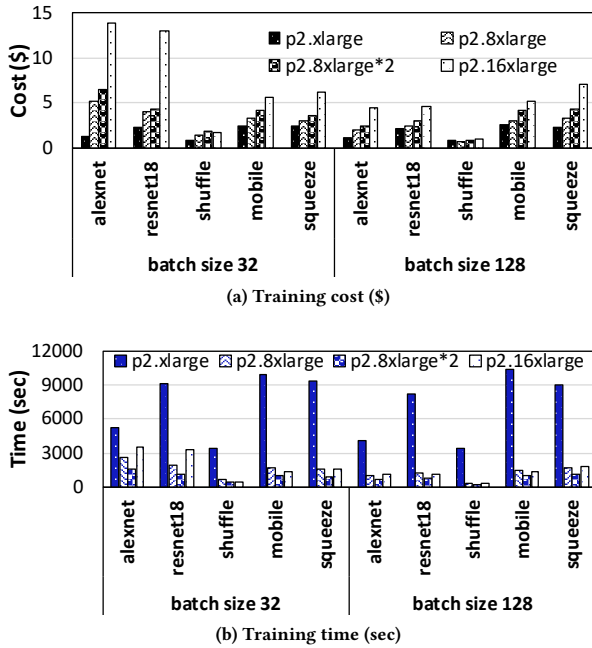


Figure 9: Training Time and Cost (P2, Small Models)

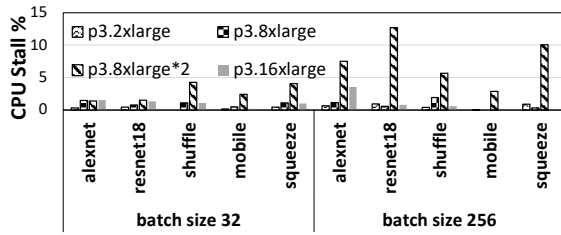
than what the 8xlarge instance can provide, training time and cost are lower when using a combination of 8xlarge instances connected via network compared to using the 16xlarge instance. For the lowest cost training, we recommend using the xlarge instance with a single GPU.

## 5.2 Analysis on AWS P3

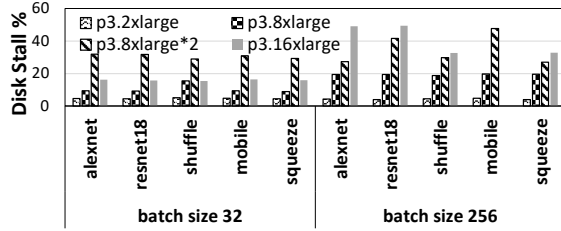
AWS P3 instances use the NVIDIA V100 GPU with NVLink interconnect as already described in section 2. The P3 instances are high performing instances capable of training large DNN models in a cost effective manner. We begin our discussion with the stall analysis of P3 in the sequel.

**5.2.1 Stall Analysis.** We show CPU and disk stalls for small models in Figure 11 and large models in Figure 12. The CPU and disk stalls follow the same pattern as in P2. The CPU stalls are negligible and the disk stall is high for the 16xlarge instance. Unlike P2.16xlarge, the P3.16xlarge has eight GPUs and hence eight workers performing I/O in the attached SSD. However, the throughput of training is also high due to the higher compute capacity (of both GPU and CPU) of the instance leading to higher usage of SSD and higher disk stalls.

The P3 instances use NVLink for communication between the GPUs instead of the PCIe bus. As discussed in section 2, NVLink offers significantly higher bandwidth compared to traditional PCIe based communication. As a result, we expect lower interconnect stalls while using NVLink. We show the interconnect stalls for P3

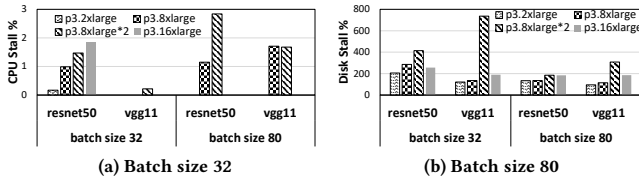


(a) CPU stall %



(b) Disk stall %

Figure 11: CPU and disk stall (P3, small models)



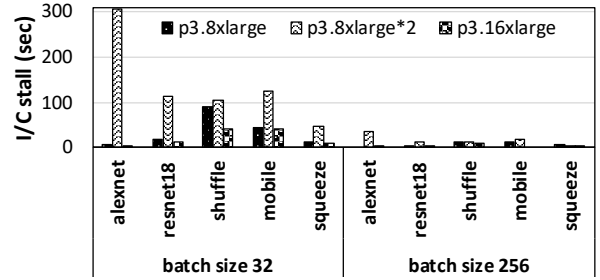
(a) Batch size 32

(b) Batch size 80

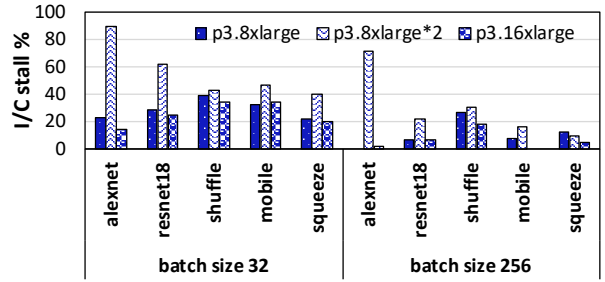
Figure 12: CPU and disk stall (P3, Large Models)

in Figure 13 and 15 and notice lower interconnect stalls than P2 instances as expected. However, we were also expecting the 8xlarge instance to have lower interconnect stall than the 16xlarge instance because there are lesser number of GPUs in the 8xlarge. As the number of GPUs decrease, the volume of gradients to be transferred (as each GPU generates gradients) also decreases requiring lesser bandwidth from the underlying interconnect. This should ideally transform into lower interconnect stalls for the 8xlarge but on the contrary we notice mostly a higher interconnect stall. So, **why do 8xlarge instances have higher interconnect stalls than 16xlarge?**

The reason for this anomaly is that although AWS provides a highly connected crossbar architecture (refer Figure 2) for communication via the NVLink, this may not be the case for the 8xlarge. Ideally, AWS should split the 16xlarge instance into two 8xlarge such that each instance gets an entire crossbar as shown by the dotted line in the Figure 2. This would have provided the tenant/user with a highly connected, high bandwidth GPU interconnect resulting in lower interconnect stalls. However, we theorize that AWS is not able to "evenly slice" the physical interconnect so as to give an entire crossbar to the 8xlarge instance. This may be due to multiple single size GPU requests from several tenants occupying GPUs in a crossbar. The 8xlarge instance loses the benefit of a crossbar architecture due to this and ends up being less performant with regard to

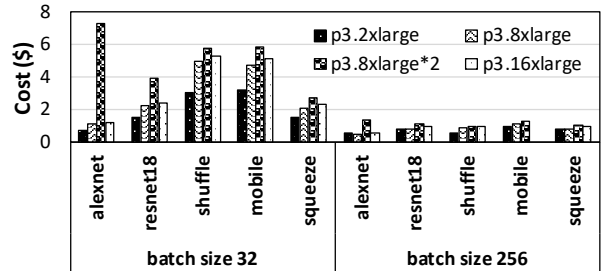


(a) Interconnect stall (sec)

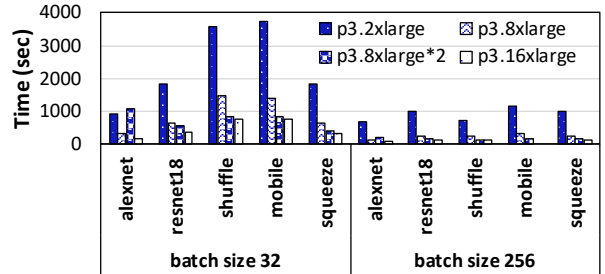


(b) Interconnect stall %

Figure 13: Interconnect stall (P3, Small models)



(a) Training cost (\$)



(b) Training time (sec)

Figure 14: Training Time and Cost (P3, Small Models)



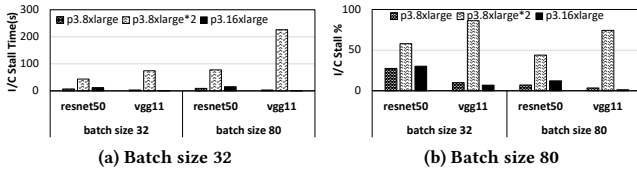


Figure 15: Interconnect stall (P3 Large Models)

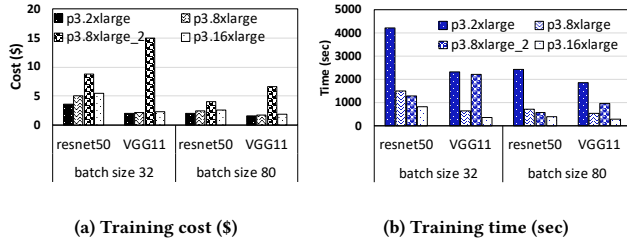


Figure 16: Training Time and Cost (P3 Large Models)

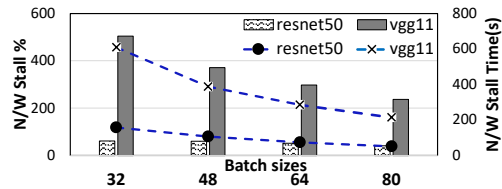


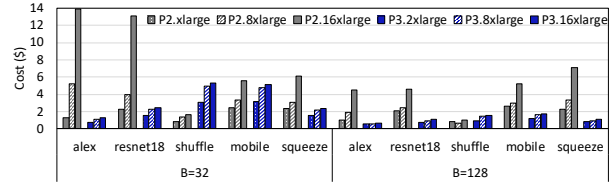
Figure 17: Network Stall of two P3.8xlarge instances

interconnect stalls. This "trait" of AWS interconnects is essentially probabilistic in nature and a tenant may indeed end up getting an entire crossbar for their 8xlarge instance resulting in lower interconnect stalls. But, **what happens when the instances are connected via the network?**

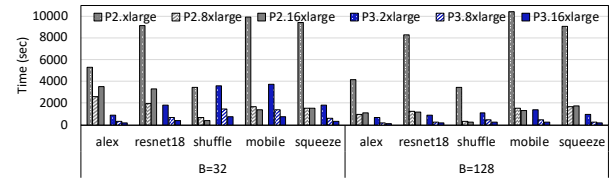
To answer this question, we calculate the network stall of two P3.8xlarge instances connected via the network (P3.8xlarge\*2) in Figure 17 as part of step ⑤ of STASH and notice network stalls as high as 500%. This is because as soon as the "all-reduce" ring contains a network link, the training gets throttled on this slow network link. Compared to NVLink interconnect which has a sufficiently large bandwidth to accommodate fast data transfers, the network link introduces higher slowdowns. This discourages us to run training over network links unless it can not be avoided due to timing SLOs.

**5.2.2 Cost Analysis.** We show the cost and run time analysis of P3 instances in Figures 14 and 16. The cost analysis follows the same pattern as in P2 instances but the performance of instances differ. We find that the smallest P3 instance, the 2xlarge is the most cost optimal followed by the 8xlarge and the 16xlarge. An immediate question that can be asked here is **how is 8xlarge more cost optimal than 16xlarge?**

The answer to this question is although 16xlarge instance has lower interconnect stalls than the 8xlarge instance, it still suffers from high disk stalls and hence ends up being less cost optimal than

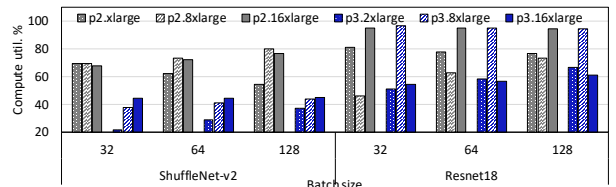


(a) Training time per epoch

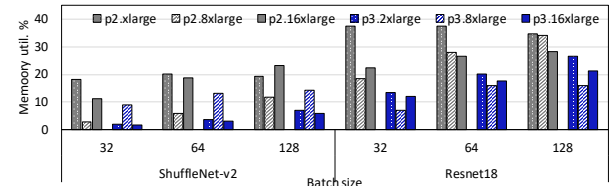


(b) Training cost per epoch

Figure 18: P2 vs P3 training time and cost comparison.



(a) GPU compute utilization



(b) GPU memory utilization

Figure 19: GPU util. of P2 vs P3 for a small & large model.

the 8xlarge. However, the 16xlarge remains the most performant instance followed by the 8xlarge and the 2xlarge. This is because the stalls in 16xlarge are not large enough to make it less performant than the 8xlarge.

Network connected instances are the costliest due to high network stalls. However they are more performant than a single instance of the same type owing to more compute resources.

**5.2.3 Recommendation.** We recommend the single 2xlarge as the most cost optimal instance for training. However, we realize that using a single GPU is not practical to train most models due to time constraints. Hence, tenants must specifically find out the stalls for their models before running an end-to-end training on an 8xlarge or a 16xlarge. Fortunately, STASH is designed to solve this very problem and tenants can use it to find out the various stalls in their model.

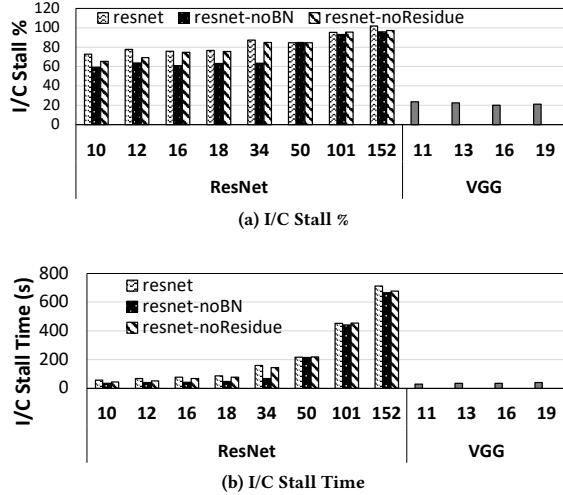


Figure 20: Interconnect stall in ResNet and VGG with increasing number of layers

### 5.3 Comparison between P2 and P3

We now compare the two GPU instance types – P2 and P3 from a cost efficiency point of view. From Figure 18, we notice that P3 instances are generally more cost optimal than P2 instances, although P3 instances are about  $3.5\times$  costlier per hour than P2 instances. This is because of the lower stalls P3 instances experience compared to P2s. However, some smaller models like ShuffleNet aren’t able to exploit the memory and compute capacity of large V100 GPUs present in the P3 instances unlike models with many layers like ResNet18 (shown in figure 19). Hence, such small models are more cost optimal on P2 instances. We also show the training throughput of various models on P2 and P3 in Figure 18.

**5.3.1 Recommendation.** While we recommend using P3 instances whenever possible, we do notice that smaller models such as SqueezeNet are more cost optimal on P2s. We also note that AWS has limited GPU availability and tenants might not always receive the desired number and type of GPUs from AWS. Thus, tenants may be forced to use P2 instances due to unavailability of P3s. We recommend using P3 instances whenever possible except for very small models.

## 6 MICRO CHARACTERIZATION, ANALYSIS AND RECOMMENDATION MODEL

In this section, we analyze the interconnect and network stalls through synthetic DNN models to (i) find characteristics in model architecture that influence interconnect and network stall behavior, and (ii) express the generality of our interconnect and network stall profiler for unseen models. Furthermore, we introduce our recommendation model that suggests a cost-optimized instance configuration on AWS, given a fixed time budget.

### 6.1 Micro Characterization

In order to verify the generality of our profiling technique for new models, we create synthetic models by altering the model architecture of popular DNNs, viz., ResNet and VGG, to highlight features that can affect stall behavior. Note that these changes are not meant

to improve the model accuracy or any other DNN feature such as convergence time. Rather, they are meant to provide insights that can be leveraged by users to architect DNN models to improve system utilization. We run all experiments on a P3.16xlarge instance with a batch size of 32 per GPU repeated thrice and the results averaged. The choice of using a smaller batch size (32) is made so as to maximize all-reduce cycles and, thereby, exacerbate communication stall behavior. We begin our discussion by asking two questions: (i) **Is there a relationship between the number of layers in a model and its communication stalls?**, and (ii) **How does the number of gradients to be transferred in a model affect communication stalls?**

**6.1.1 Relationship between DNN layers, gradients and communication stalls.** We answer the above questions by observing the communication stalls of ResNet and VGG with varying number of layers (Figures 20 and 21). We observe that as the number of layers increase (accompanied by a commensurate increase in the number of gradients), both the interconnect stall and network stall time increases. This is expected, as there is more data to be transferred with the increase in number of gradients. However, despite the number of gradients in VGG being far more than that in ResNet, *VGG is observed to have lower interconnect stall time than ResNet (Figure 20)*. Moreover, we also notice that *the network stall time of VGG is significantly more than ResNet (Figure 21)*. These facts lead us to the next question that arises logically: **Why is the interconnect stall time of VGG low and the network stall time high when compared to ResNet?**

**6.1.2 Explaining VGG communication stalls.** From [38], we know that distributed PyTorch overlaps communication and computation during the backward pass. At every layer, there is a synchronization point where communication takes place between the workers. In case of ResNet, there is a large number of layers and relatively fewer gradients to transfer per layer. In comparison, VGG has fewer layers, but a larger number of gradients to transfer per layer. VGG16 consists of about 134.7 million trainable parameters while ResNet152 consists of only 58.5 million [35]. Therefore, the gradients to transfer per synchronization point is greater in VGG, but the number of times the gradients get transferred is higher in ResNet. We now explain how this characteristic leads to the interconnect stalls observed in the previous subsection.

Suppose VGG has  $G_{vgg}$  gradients and  $L_{vgg}$  layers, and ResNet has  $G_{res}$  gradients and  $L_{res}$  layers. Also, let us say that NVLink offers  $B_{nv}$  bandwidth with  $\tau_{nv}$  latency. The time to transfer gradients comprises both latency and data transfer time. Define this for VGG and ResNet to respectively be  $T_{vgg}$  and  $T_{res}$ . Thus, the transfer time using NVLink is given by:

$$T_{vgg} = \left[ \tau_{nv} + \frac{G_{vgg}}{L_{vgg} \times B_{nv}} \right] \times L_{vgg}, T_{res} = \left[ \tau_{nv} + \frac{G_{res}}{L_{res} \times B_{nv}} \right] \times L_{res}$$

Since NVLink offers very high bandwidth (more than 100 Gbps [36]), and also because both models have a large number of layers, we can assume  $\frac{G_{vgg}}{L_{vgg} \times B_{nv}} \ll \tau_{nv}$  and  $\frac{G_{res}}{L_{res} \times B_{nv}} \ll \tau_{nv}$ . Hence, data transfer time over NVLink is  $T_{vgg} \approx \tau_{nv} \times L_{vgg}$  and  $T_{res} \approx \tau_{nv} \times L_{res}$ .

$$\text{Thus, } L_{res} > L_{vgg} \implies T_{res} > T_{vgg}$$

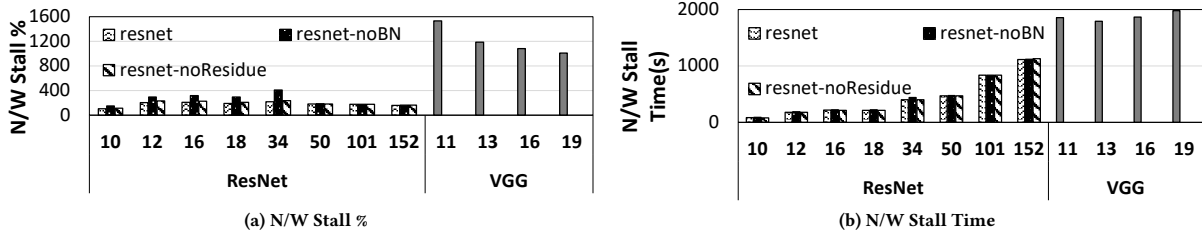


Figure 21: Network stall in ResNet and VGG with increasing number of layers.

In other words, the training process experiences increased slowdown due to the larger number of layers to transfer in ResNet (or in any other deep model, for that matter). It follows that in the case of VGG, although the data to be transferred is much larger, the time to transfer is nearly zero due to the lower number of layers. The only slowdown we observe here is due to the transfer latency associated with the transfer link/framework.

Now, we explain the high network stall time observed for VGG in the previous subsection. As already explained in section 4.2.2, the collective all-reduce performed across the network-connected instances is throttled by the network link. Hence, we can assume that the data transfer time is a function of the network link only. Suppose the network link offers  $B_{nw}$  bandwidth with  $\tau_{nw}$  latency. Similarly, the data transfer time over network is:

$$T_{vgg} = \left[ \tau_{nw} + \frac{G_{vgg}}{L_{vgg} \times B_{nw}} \right] \times L_{vgg}, T_{res} = \left[ \tau_{nw} + \frac{G_{res}}{L_{res} \times B_{nw}} \right] \times L_{res}$$

Since the network link is slow, we can assume  $\tau_{nw} \ll \frac{G_{vgg}}{B_{nw}}$  and  $\tau_{nw} \ll \frac{G_{res}}{B_{nw}}$ . Hence, the data transfer time over NVLink is  $T_{vgg} \approx \frac{G_{vgg}}{B_{nw}}$  and  $T_{res} \approx \frac{G_{res}}{B_{nw}}$ .

$$\text{Thus, } \boxed{G_{vgg} > G_{res} \implies T_{vgg} > T_{res}}$$

In other words, since the network link is slow, the data transfer is throttled on the transfer time rather than the latency. Since a much larger volume of gradients needs to be transferred in VGG (in total), the network stall is much higher in VGG than in ResNet.

**6.1.3 Impact of model architecture.** To probe further into the specific aspects of DNN model architecture that impact interconnect stalls, we made two changes to the ResNet model by removing batch normalization (BN) as well as residual networks. These changes are intended to show the extent to which these layer types impact communication stalls. From Figures 20 and 21, we notice that removing residual networks has minimal impact on communication overhead. This is because residual networks do not introduce any new layers and hence do not impact communication. However, removing BN reduces the number of layers in the model and hence we see changes in communication stall in the figures.

**6.1.4 Recommendation.** From our experiments, we observe that models with very deep networks are unable to fully exploit the fast

NVLink interconnect, whereas shallower networks with large gradient transfers can be throttled on the network link. Hence, we recommend running shallow networks with large gradients on instances with the best interconnect possible. However, if the model is very deep, the models can be run on instances without the best interconnect, such as the P3.8xlarge. The penalty for running such models on network-connected instances is also minimized. Note that models can be made more complex through residual connections without affecting communication time whereas removing batch normalization decreases the number of layers effecting communication.

## 6.2 Recommendation model

In this section we describe our recommendation model that suggests a cost optimal cluster configuration (the number and type of public cloud GPU instance), given a fixed time budget ( $T$ ) and the expected number of epochs (to converge) from the user<sup>4</sup>. We describe our problem as:

$$\min \sum_{instance\ i=1}^n training\_cost\_i \quad s.t. \quad training\_time < T$$

The user is expected to run STASH on the instance with the largest number of GPUs ( $GPU_{large}$ ) of the public cloud to find the interconnect stall. Along with this, two network-connected instances with half the number of  $GPU_{large}$  each are to be profiled to find the network stalls (refer section 4). We do not expect the user to run STASH on all GPU instance sizes, but the recommendation model is specific to a GPU instance family (P2, P3, etc.). The recommendation model uses the single epoch time from the largest GPU instance and finds the expected training time by multiplying it with the number of epochs the user intends to run. It then determines whether the number of GPUs in the cluster needs to be increased (scale up) or decreased (scale down) based on whether the expected training time meets or violates the budget SLO.

Now, let's suppose that the model found that the number of GPUs in the cluster must be increased to decrease training time. In order to do this, we derive below a simple equation to find the expected training time based on the number of GPUs in the cluster with at least two different instances.

Let's say  $\mu_{old}$  is the training throughput (training samples/s) using a single instance with a maximal number  $GPU_{large}$  of GPUs. Let  $GPU_{cluster} > GPU_{large}$  is the total number of GPUs in a cluster of instances. We estimate the new training throughput of the cluster

<sup>4</sup>Again, one could alternatively minimize execution time given a monetary cost budget.

$\mu_{new}$  and training time  $train\_time$  over  $n$  samples as:

$$\mu_{new} = \mu_{old} + \frac{\mu_{old}}{GPU_{large}} \times GPU_{cluster} \quad train\_time = \frac{n}{\mu_{new}}$$

Now, let's say from our profiling, we find the network stall in this particular DNN model to be  $stall_{nw}$  as a percentage of  $train\_time$ . Hence, there will be a one time penalty of  $stall_{nw}$  in addition to the total running time.

$$total\_train\_time = train\_time + \frac{stall_{nw}}{100} \times train\_time \quad (1)$$

Next, let us suppose that the user is not exceeding the time budget when using the largest GPU instance. We will now derive the total training time by using an instance with lesser GPUs than what was used in profiling. Let's say from our profiling, we find interconnect stall time in this particular DNN model to be  $t_{ic}$ . Hence the actual compute time  $t_{comp} = train\_time - t_{ic}$ .

In order to scale down the GPUs, we will make a simplifying assumption that the throughput scales down linearly with the number of GPUs. We do this to avoid profiling every instance type on the public cloud. Hence, considering we profiled on the largest instance with  $GPU_{large}$  number of GPUs, the new training time for the scaled down machine with  $GPU_{small}$  number of GPUs would be

$$total\_train\_time = \frac{GPU_{large}}{GPU_{small}} \times train\_time \quad (2)$$

However, if  $GPU_{small} = 1$  the interconnect stall will be zero and the new training time will therefore be

$$total\_train\_time = GPU_{large} \times t_{comp} \quad (3)$$

We now propose a greedy approximation algorithm to use equations (1), (2) and (3).

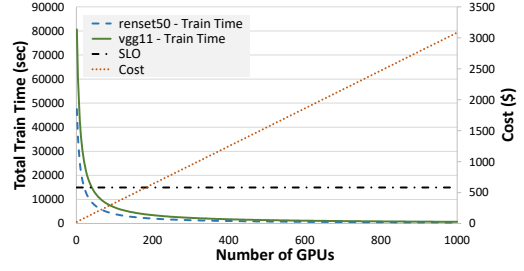


**Figure 22: Expected training time projected by recommendation model.**

#### Algorithm Scale Up and Scale Down

**Input:**  $train\_time\_bgt, stall\_ic, stall\_nw, gpu\_large, n, t_{comp}, instances\_list$   
**Output:** Type and number of instances

**Initialization:** set  $D = \{\}$ ,  $instance\_gpus$  = list of instances sorted on number of GPUs,  $largest\_instance$  = instance with largest number of GPUs

```

1: function SCALE_UP
2:   deficit_time = train_time - train_time_bgt
3:   while deficit_time > 0 do
4:     D[largest_instance] += 1
5:     for instance in instance_gpus do
6:       Use equation (1)
7:       deficit_time = train_time - train_time_bgt
8:       if deficit_time < 0 then
9:         D[instance] += 1
10:        break
11:  return D
12: function SCALE_DOWN
13:   best_instance = largest_instance
14:   for instance in instance_gpus do
15:     gpus = GPUs in instance
16:     if gpus > 1 then
17:       Use equation (2)
18:     else
19:       Use equation (3)
20:     if train_time < train_time_bgt then
21:       best_instance = instance
22:     else
23:       break
24:
25:   D[best_instance] += 1
26:  return D

```

The algorithm consists of two functions – SCALE\_UP() and SCALE\_DOWN(), to increase or decrease the number of GPUs in the cluster, respectively, to meet the timing budget. The algorithm takes as input all variables in the RHS of equations (1), (2), (3) and the instances to be considered for scaling up/down. Note that the profiling runs on the instance with the largest number of GPUs, and the model scales up or down the number of GPUs from  $GPU_{large}$ . We simulate the output of SCALE\_UP() in Figure 22 and we see how the number of GPUs can be scaled up to lower the training time. The algorithm will greedily choose the cheapest instances to fulfill the timing SLO (accounting for the network stall from our profiler), thereby lowering the training cost. For SCALE\_DOWN(), the algorithm simply picks up instances with lower number of GPUs if the lower throughput can still honor the time budget.

## 7 RELATED WORK

This section discusses related work pertaining to deep learning characterization in addition to covering specific works in DDL that focus on reducing communication overhead and performing cost optimization in the public cloud.

**Characterizing Deep Learning.** There is a wealth of existing work in the area of deep learning characterization [3, 4, 25, 29, 39, 42, 44, 45, 57, 62, 64, 66]. In [64], the authors analyze two months of MLaaS production data in Alibaba cloud [2] and provide insights into its cluster scheduling and low GPU utilization. [62] characterizes deep learning workloads on the Alibaba-PAI platform [10] and in [39], the authors build a measurement and prediction framework to train convolution neural networks with transient VMs.

**Optimizing DDL communication.** [38, 53] aim to reduce communication time by overlapping it with compute. [13, 15, 21, 22, 24, 30, 37, 40, 41, 49, 56, 61, 68, 69] are proposed algorithmic changes to reduce communication time in DDL. These work do not optimize the underlying system being used. [54, 55] are simulation platforms to measure and build new communication based algorithms for DDL. However, they are agnostic about the underlying hardware induced delays.

**Cost optimization in the public cloud.** Public cloud providers offer cost management tools that enables tenants to monitor and optimize their cloud-spend [65]. e.g., [51]. Prior work such as, e.g., [9, 17, 67] explicitly focus on reducing costs of migrating and running "generic" workloads on public cloud (including DNN inference), i.e., not specifically deep learning. Some of this work is described as efficient resource management, which may not explicitly discuss monetary costs, but implicitly does. For example, the use of serverless functions (e.g., Amazon Lambda) for (not stateful) microservice-based applications is a cost-based choice because serverless functions have a finer pricing granularity, shorter (warm start) spin-up times, and less management overhead compared to virtual machines, e.g., [60] (even though their cost per unit-resource per unit time is higher). Note DDL is obviously quite stateful. Also, prior work, e.g., [19], has applied deep learning to the problem of efficient resource management.

## 8 CONCLUDING REMARKS

To summarize, we introduce a DDL stall profiler STASH and present novel methodologies to measure the interconnect and network stall in DDL training. Using the profiler, we extensively characterize AWS P type instances for the various stalls they suffer from while running popular DNNs. We find communication stall to be the major bottleneck in DDL training and that AWS instances suffer heavily from communication stalls. The observed interconnect stalls and network stalls were up to 90% and 500% respectively. The reasoning for these high stalls were stated to be severe bandwidth contention when using the PCIe bus and sub-optimal resource allocation when using the NVLink. The high stall numbers directly translated to higher training cost compared to instances with lower communication stalls. Further, we explain through modelling how certain DNN model architecture features (layers and gradient size) drive communication stall behavior, and how users can modify their model architecture to lower communication stalls. And finally, we propose a recommendation model which can be used by users to build a cost optimal compute cluster for training their model.

Note that while our experiments are run on AWS, the methods described herein are generic and can be applied on any public cloud. Users can characterize any public cloud provider of their choosing using the proposed methodology and reduce their training cost.

## REFERENCES

- [1] Martín Abadi, Paul Barham, Jianmin Chen, Zhifeng Chen, Andy Davis, Jeffrey Dean, Matthieu Devin, Sanjay Ghemawat, Geoffrey Irving, Michael Isard, Manjunath Kudlur, Josh Levenberg, Rajat Monga, Sherry Moore, Derek G. Murray, Benoit Steiner, Paul Tucker, Vijay Vasudevan, Pete Warden, Martin Wicke, Yuan Yu, and Xiaoqiang Zheng. TensorFlow: A System for Large-scale Machine Learning. In *Proc. USENIX OSDI*, 2016.
- [2] Alibaba Cloud. <https://www.alibabacloud.com/>, Accessed: 2022.06.15.
- [3] Ammar Ahmad Awan, Jereon Bédorf, Ching-Hsiang Chu, Hari Subramoni, and Dhableswar K Panda. Scalable distributed DNN training using TensorFlow and CUDA-aware MPI: Characterization, designs, and performance evaluation. In *Proc. IEEE/ACM CCGRID*, 2019.
- [4] Ammar Ahmad Awan, Hari Subramoni, and Dhableswar K Panda. An in-depth performance characterization of CPU-and GPU-based DNN training on modern architectures. In *Proceedings of the Machine Learning on HPC Environments*, 2017.
- [5] Amazon Web Services (AWS). <https://aws.amazon.com/>, 2022.06.08.
- [6] AWS NVIDIA GPU instances. <https://aws.amazon.com/nvidia/>, Accessed: 2022.06.08.
- [7] AWS HPC. <https://aws.amazon.com/hpc/>, Accessed: 2022-06-08.
- [8] Azure HPC. <https://azure.microsoft.com/en-us/solutions/high-performance-computing/#overview>, Accessed: 2022-06-08.
- [9] Ataollah Fatahi Baarzi, George Kesidis, Carlee Joe-Wong, and Mohammad Shahrad. On merits and viability of multi-cloud serverless. In *Proceedings of the ACM Symposium on Cloud Computing*, pages 600–608, 2021.
- [10] Alibaba PAI. <https://github.com/AlibabaPAI>, Accessed: 2022.06.15.
- [11] DawnBench. <https://dawn.cs.stanford.edu/benchmark/>, Accessed: 2022-06-08.
- [12] Jeffrey Dean, Greg Corrado, Rajat Monga, Kai Chen, Matthieu Devin, Mark Mao, Marc' aurelio Ranzato, Andrew Senior, Paul Tucker, Ke Yang, Quoc Le, and Andrew Ng. Large scale distributed deep networks. In F. Pereira, C.J. Burges, L. Bottou, and K.Q. Weinberger, editors, *Advances in Neural Information Processing Systems*, volume 25. Curran Associates, Inc., 2012.
- [13] Jeffrey Dean, Greg Corrado, Rajat Monga, Kai Chen, Matthieu Devin, Mark Mao, Marc' aurelio Ranzato, Andrew Senior, Paul Tucker, Ke Yang, Quoc Le, and Andrew Ng. Large scale distributed deep networks. In *Proc. Advances in Neural Information Processing Systems*, volume 25, 2012.
- [14] Jacob Devlin, Ming-Wei Chang, Kenton Lee, and Kristina Toutanova. BERT: Pre-training of Deep Bidirectional Transformers for Language Understanding. <https://arxiv.org/abs/1810.04805>, 24 May 2019.
- [15] Jianbo Dong, Zheng Cao, Tao Zhang, Jianxi Ye, Shaochuang Wang, Fei Feng, Li Zhao, Xiaoyong Liu, Liuyihan Song, Liwei Peng, et al. Eflops: Algorithm and system co-design for a high performance distributed training platform. In *2020 IEEE International Symposium on High Performance Computer Architecture (HPCA)*, pages 610–622. IEEE, 2020.
- [16] DS-Analyzer. <https://github.com/msr-fiddle/DS-Analyzer>, Accessed: 2022.06.08.
- [17] Tarek Elgamal, A. Sandur, K. Nahrstedt, and G. Agha. Costless: Optimizing Cost of Serverless Computing through Function Fusion and Placement. In *IEEE/ACM Symposium on Edge Computing (SEC)*, pages 300–312, Seattle, WA, USA, Oct. 25–27, 2018.
- [18] Jeremy Fowers and al. A Configurable Cloud-Scale DNN Processor for Real-Time AI. In *Proc. ACM ISCA*, June 2018.
- [19] Yu Gan, Yanqi Zhang, Kelvin Hu, Dailun Cheng, Yuan He, Meghna Pancholi, and Christina Delimitrou. Leveraging Deep Learning to Improve Performance Predictability in Cloud Microservices with Seer. *ACM SIGOPS Operating Systems Review*, 53(1), July 2019.
- [20] Google Cloud : Cloud Computing Services. <https://cloud.google.com/>, Accessed: 2022.06.15.
- [21] Priya Goyal, Piotr Dollár, Ross Girshick, Pieter Noordhuis, Lukasz Wesolowski, Aapo Kyrola, Andrew Tulloch, Yangqing Jia, and Kaiming He. Accurate, large minibatch SGD: Training ImageNet in 1 hour. *arXiv preprint arXiv:1706.02677*, 2017.
- [22] Sayed Hadi Hashemi, Sangeetha Abdu Jyothi, and Roy Campbell. Tictac: Accelerating distributed deep learning with communication scheduling. *Proceedings of Machine Learning and Systems*, 1:418–430, 2019.
- [23] Kaiming He, Xiangyu Zhang, Shaoqing Ren, and Jian Sun. Identity mappings in deep residual networks. In Bastian Leibe, Jiri Matas, Nicu Sebe, and Max Welling, editors, *Computer Vision – ECCV 2016*, 2016.
- [24] Qirong Ho, James Cipar, Henggang Cui, Jin Kyu Kim, Seunghak Lee, Phillip B. Gibbons, Garth A. Gibson, Gregory R. Ganger, and Eric P. Xing. More effective distributed ml via a stale synchronous parallel parameter server. In *Proc. NIPS*, 2013.
- [25] Qinghao Hu, Peng Sun, Shengen Yan, Yonggang Wen, and Tianwei Zhang. Characterization and prediction of deep learning workloads in large-scale GPU datacenters. In *Proceedings of the International Conference for High Performance Computing, Networking, Storage and Analysis*, pages 1–15, 2021.
- [26] Yu Huang and Yue Chen. Autonomous driving with deep learning: A survey of state-of-art technologies. <https://arxiv.org/abs/2006.06091>, 2020.



- [27] Forrest N. Iandola, Song Han, Matthew W. Moskewicz, Khalid Ashraf, William J. Dally, and Kurt Keutzer. SqueezeNet: AlexNet-level accuracy with 50x fewer parameters and <0.5MB model size. <https://arxiv.org/abs/1602.07360>, 2016.
- [28] Imagenet 1K. <https://image-net.org/challenges/LSVRC/2012/>.
- [29] Arpan Jain, Ammar Ahmad Awan, Quentin Anthony, Hari Subramoni, and Dhableswar K DK Panda. Performance characterization of dnn training using tensorflow and pytorch on modern clusters. In *2019 IEEE International Conference on Cluster Computing (CLUSTER)*, pages 1–11. IEEE, 2019.
- [30] Anand Jayarajan, Jinliang Wei, Garth Gibson, Alexandra Fedorova, and Gennady Pekhimenko. Priority-based parameter propagation for distributed DNN training. *Proceedings of Machine Learning and Systems*, 1:132–145, 2019.
- [31] D. Jurafsky and J.H. Martin. *Speech and Language Processing* (3rd ed. draft). <https://web.stanford.edu/~jurafsky/slp3/>, Dec 29, 2021.
- [32] Rashika Kheria, Purna Sanyal, Sr. James Jeun, and Amr Ragab. Optimizing deep learning on P3 and P3dn with EFA. <https://aws.amazon.com/blogs/compute/optimizing-deep-learning-on-p3-and-p3dn-with-efa/>, Accessed: 2022.06.08.
- [33] Yunyong Ko, Kibong Choi, Jiwon Seo, and Sang-Wook Kim. An in-depth analysis of distributed training of deep neural networks. In *2021 IEEE International Parallel and Distributed Processing Symposium (IPDPS)*, pages 994–1003. IEEE, 2021.
- [34] Alex Krizhevsky, Ilya Sutskever, and Geoffrey E Hinton. Imagenet classification with deep convolutional neural networks. In *Advances in Neural Information Processing Systems*, volume 25, 2012.
- [35] Mei Leong, Dilip Prasad, Yong Tsui Lee, and Feng Lin. Semi-cnn architecture for effective spatio-temporal learning in action recognition. *Applied Sciences*, 10:557, 01 2020.
- [36] Ang Li, Shuaiwen Leon Song, Jieyang Chen, Jiajia Li, Xu Liu, Nathan R Tallent, and Kevin J Barker. Evaluating modern GPU interconnect: PCIe, NVLink, NV-SLI, NVSwitch and GPUDirect. *IEEE Transactions on Parallel and Distributed Systems*, 31(1):94–110, 2019.
- [37] Mu Li, David G. Andersen, Jun Woo Park, Alexander J. Smola, Amr Ahmed, Vanja Josifovski, James Long, Eugene J. Shekita, and Bor-Yiing Su. Scaling distributed machine learning with the parameter server. In *Proc. USENIX OSDI*, 2014.
- [38] Shen Li, Yanli Zhao, Rohan Varma, Omkar Salpekar, Pieter Noordhuis, Teng Li, Adam Paszke, Jeff Smith, Brian Vaughan, Pritam Damania, and Soumith Chintala. PyTorch Distributed: Experiences on Accelerating Data Parallel Training. *Proc. VLDB Endow.*, 13(12):3005–3018, Aug 2020.
- [39] Shijian Li, Robert J Walls, and Tian Guo. Characterizing and modeling distributed training with transient cloud GPU servers. In *Proc. IEEE 40th International Conference on Distributed Computing Systems (ICDCS)*, pages 943–953, 2020.
- [40] Xiangru Lian, Wei Zhang, Ce Zhang, and Ji Liu. Asynchronous decentralized parallel stochastic gradient descent. In *International Conference on Machine Learning*, pages 3043–3052. PMLR, 2018.
- [41] Yujun Lin, Song Han, Huizi Mao, Yu Wang, and William J Dally. Deep gradient compression: Reducing the communication bandwidth for distributed training. *arXiv preprint arXiv:1712.01887*, 2017.
- [42] Jie Liu, Jiawen Liu, Wan Du, and Dong Li. Performance analysis and characterization of training deep learning models on mobile device. In *2019 IEEE 25th International Conference on Parallel and Distributed Systems (ICPADS)*, pages 506–515. IEEE, 2019.
- [43] Ningning Ma, Xiangyu Zhang, Hai-Tao Zheng, and Jian Sun. Shufflenet v2: Practical guidelines for efficient cnn architecture design. In *Proceedings of the European Conference on Computer Vision (ECCV)*, September 2018.
- [44] Jayashree Mohan, Amar Phanishayee, Ashish Raniwala, and Vijay Chidambaram. Analyzing and mitigating data stalls in dnn training. <https://arxiv.org/abs/2007.06775>, 2021.
- [45] Saiful A Mojumder, Marcia S Louis, Yifan Sun, Amir Kavayan Ziabari, José L Abellán, John Kim, David Kaeli, and Ajay Joshi. Profiling DNN workloads on a Volta-based DGX-1 system. In *Proc. IEEE International Symposium on Workload Characterization (IISWC)*, pages 122–133. IEEE, 2018.
- [46] Microsoft Azure. <https://azure.microsoft.com/>, 2022.06.08.
- [47] Project Fiddle. <https://aka.ms/msr-fiddle>, Accessed: 2022-06-08.
- [48] Deepak Narayanan, Aaron Harlap, Amar Phanishayee, Vivek Seshadri, Nikhil R. Devanur, Gregory R. Ganger, Phillip B. Gibbons, and Matei Zaharia. PipeDream: Generalized Pipeline Parallelism for DNN Training. In *Proc. SOSP*, 2019.
- [49] NCCL. <https://developer.nvidia.com/nccl>, Accessed: 2022.06.15.
- [50] NVIDIA Deep Learning Examples for Tensor Cores. <https://github.com/NVIDIA/DeepLearningExamples>, Accessed: 2022.06.08.
- [51] Optimize your Azure costs. <https://azure.microsoft.com/en-us/overview/cost-optimization/>.
- [52] N.J. Parmar, A. Vaswani, J. Uszkoreit, L. Kaiser, N. Shazeer, A. Ku, and D. Tran. Image Transformer. In *Proc. International Conference on Machine Learning (ICML)*, 2018.
- [53] Saeed Rashidi, Matthew Denton, Srinivas Sridharan, Sudarshan Srinivasan, Amoghavarsha Suresh, Jade Nie, and Tushar Krishna. Enabling compute-communication overlap in distributed deep learning training platforms. In *Proc. ACM/IEEE ISCA*, pages 540–553, 2021.
- [54] Saeed Rashidi, Pallavi Shurpali, Srinivas Sridharan, Naader Hassani, Dheevatsa Mudigere, Krishnakumar Nair, Misha Smelyanski, and Tushar Krishna. Scalable distributed training of recommendation models: An Astra-Sim+ ns3 case-study with TCP/IP transport. In *2020 IEEE Symposium on High-Performance Interconnects (HOTI)*, pages 33–42. IEEE, 2020.
- [55] Saeed Rashidi, Srinivas Sridharan, Sudarshan Srinivasan, and Tushar Krishna. Astra-Sim: Enabling SW/HW co-design exploration for distributed DL training platforms. In *Proc. IEEE International Symposium on Performance Analysis of Systems and Software (ISPASS)*, pages 81–92, 2020.
- [56] Saeed Rashidi, William Won, Sudarshan Srinivasan, Srinivas Sridharan, and Tushar Krishna. Themis: A network bandwidth-aware collective scheduling policy for distributed training of DL models. In *Proc. ACM/IEEE ISCA*, pages 581–596, 2022.
- [57] Ananda Samajdar, Jan Moritz Joseph, Yuhao Zhu, Paul Whatmough, Matthew Mattina, and Tushar Krishna. A systematic methodology for characterizing scalability of DNN accelerators using scale-sim. In *Proc. IEEE International Symposium on Performance Analysis of Systems and Software (ISPASS)*, pages 58–68, 2020.
- [58] Mark Sandler, Andrew Howard, Menglong Zhu, Andrey Zhmoginov, and Liang-Chieh Chen. Mobilenetv2: Inverted residuals and linear bottlenecks. In *2018 IEEE/CVF Conference on Computer Vision and Pattern Recognition*, pages 4510–4520, 2018.
- [59] Karen Simonyan and Andrew Zisserman. Very deep convolutional networks for large-scale image recognition. In *Proc. ICLR*, San Diego, CA, May 7-9, 2015.
- [60] M. Villamizar, O. Garcés, L. Ochoa, H. Castro, L. Salamanca, M. Verano, R. Casallas, S. Gil, C. Valencia, A. Zambrano, and M. Lang. Infrastructure Cost Comparison of Running Web Applications in the Cloud Using AWS Lambda and Monolithic and Microservice Architectures. In *Proc. IEEE/ACM CCGrid*, 2016.
- [61] Guanhua Wang, Amar Phanishayee, Shivaram Venkataraman, and Ion Stoicac. Blink: A fast nvlink-based collective communication library. In *Proc. Conf. Syst. Mach. Learn.*, 2018.
- [62] Mengdi Wang, Chen Meng, Guoping Long, Chuan Wu, Jun Yang, Wei Lin, and Yangqing Jia. Characterizing deep learning training workloads on Alibaba-PAI. In *Proc. IEEE Int'l Symp. on Workload Characterization (IISWC)*, pages 189–202, 2019.
- [63] Yu Wang, Gu-Yeon Wei, and David Brooks. Benchmarking TPU, GPU, and CPU Platforms for Deep Learning. <http://arxiv.org/abs/1907.10701>, 2019.
- [64] Qizhen Weng, Wencong Xiao, Yinghao Yu, Wei Wang, Cheng Wang, Jian He, Yong Li, Liping Zhang, Wei Lin, and Yu Ding. MLaaS in the Wild: Workload Analysis and Scheduling in {Large-Scale} Heterogeneous GPU Clusters. In *Proc. USENIX NSDI*, pages 945–960, 2022.
- [65] B. Whittle. Navigating Economic Uncertainty in 2020: Cutting Cloud Costs. <https://www.apptio.com/blog/navigating-economic-uncertainty-in-2020-cost-cutting-cloud/>, April 6, 2020.
- [66] Chunwei Xia, Jiacheng Zhao, Huimin Cui, and Xiaobing Feng. Characterizing dnn models for edge-cloud computing. In *2018 IEEE International Symposium on Workload Characterization (IISWC)*, pages 82–83, 2018.
- [67] Chengliang Zhang, Minchen Yu, Wei Wang, and Feng Yan. MARk: Exploiting Cloud Services for Cost-Effective, SLO-Aware Machine Learning Inference Serving. In *Proc. USENIX ATC*, Renton, WA, 2019.
- [68] Hao Zhang, Zeyu Zheng, Shizhen Xu, Wei Dai, Qirong Ho, Xiaodan Liang, Zhiting Hu, Jinliang Wei, Pengtao Xie, and Eric P Xing. Poseidon: An efficient communication architecture for distributed deep learning on GPU clusters. In *Proc. USENIX ATC*, 2017.
- [69] Sixin Zhang, Anna E Choromanska, and Yann LeCun. Deep learning with elastic averaging SGD. *Proc. Advances in neural information processing systems*, 28, 2015.